Interface pinning and slow ordering kinetics on infinitely ramified fractal structures

Umberto Marini Bettolo Marconi

Dipartimento di Matematica e Fisica, Università di Camerino, Via Madonna delle Carceri, I-62032, Camerino, Italy;
Istituto Nazionale di Fisica della Materia, Sezione di Camerino, Camerino, Italy;
and Istituto Nazionale di Fisica Nucleare, Sezione di Perugia, Perugia, Italy
(Received 28 July 1997)

We investigate the time-dependent Ginzburg-Landau (TDGL) equation for a nonconserved order parameter on an infinitely ramified (deterministic) fractal lattice employing two alternative methods: the auxiliary field approach and a numerical method of integration of the equations of evolution. In the first case the domain size evolves with time as $L(t) \sim t^{1/d_w}$, where d_w is the anomalous random-walk exponent associated with the fractal and differs from the normal value 2, which characterizes all Euclidean lattices. Such a power-law growth is identical to the one observed in the study of the spherical model on the same lattice, but fails to describe the asymptotic behavior of the numerical solutions of the TDGL equation for a scalar order parameter. In fact, the simulations performed on a two dimensional Sierpinski carpet indicate that, after an initial stage dominated by a curvature reduction mechanism in the manner of Allen and Cahn [Acta. Metall. **27**, 1085 (1979)], the system enters in a regime where the domain walls between competing phases are pinned by lattice defects. The lack of translational invariance determines a rough free-energy landscape, the existence of many metastable minima, and the suppression of the marginally stable modes, which in translationally invariant systems lead to power-law growth and self-similar patterns. On fractal structures, as the temperature vanishes the evolution is frozen since only thermally activated processes can sustain the growth of pinned domains.
[S1063-651X(98)01302-6]

PACS number(s): 64.60.Ht, 61.20.Gy, 64.60.Kw

I. INTRODUCTION

The study of the relaxation dynamics of a system initially in thermal equilibrium and abruptly rendered unstable by a sudden change of a controlling field has recently drawn considerable attention, not only because many physical properties may depend on the way a material reaches the equilibrium state, but also because it poses intriguing problems to the theory such as broken ergodicity, aging, and dynamical scaling [1]. After the quench, i.e., a rapid lowering of the temperature below the critical point of a phase-separating system, the initial, disordered state loses stability and the system undergoes a coarsening process, during which the domains corresponding to different equilibrium phases compete to grow in magnitude. About twenty years ago, Allen and Cahn [2] realized that when the order parameter is nonconserved, the driving force towards equilibrium stems from the tendency of the system to reduce the curvature of the domain walls and showed that the typical size of the domains L increases in time with a power-law behavior $L(t) \sim t^{1/2}$. In spite of the fact that the theory of phase ordering in homogeneous systems is fairly well understood, only recently the ordering kinetics on nontranslationally invariant fractal lattices has become a subject of investigation.

The present author in collaboration with Petri [3,4] considered the role of deterministic fractal supports, with finite and infinite order of ramification, on the ordering process employing the so-called spherical model, which has the advantage of rendering analytical approaches possible. It was found by means of an explicit solution that the spherical model on fractal lattices of finite order of ramification, such as the Sierpinski gasket of arbitrary embedding dimension, does not display a finite-temperature phase transition; on the

contrary, on Sierpinski carpets, whose order of ramification is infinite [5,6], there exist an order-disorder transition provided that the spectral dimension d_s exceeds the critical value 2 [7], in accord with the Mermin-Wagner theorem [8].

Interestingly, the study of the spherical model with a nonconserved order parameter has revealed the existence, even on fractals, of a characteristic length scale $L(t)$, which increases in time in a powerlike fashion $L(t) \sim t^{1/z}$, and of dynamical scaling for the correlation functions. Such a dynamical exponent z takes the value $d_w = \ln(d+3)/\ln(2)$ on Sierpinski gaskets of arbitrary embedding dimension d and $d_w \simeq 2.10$ on the planar Sierpinski carpet, where d_w is the random-walk exponent. These values of z differ from the Allen-Cahn universal value $z=2$, which characterizes the diffusive domain growth on standard lattices. We have shown [3] that in order to fully characterize the static and dynamical properties of the spherical model on fractal lattices two more quantities are required: (i) the fractal dimension d_f and (ii) the spectral dimension d_s, which for many lattices are related to d_w via the Alexander-Orbach [9] relation

$$d_w = \frac{2 d_f}{d_s}.$$

Unfortunately, the analytically soluble spherical model does not yield predictions that can be extrapolated to the physically interesting case of the scalar order parameter. In fact, the lack of sharp, well-defined interfaces between different phases renders the spherical model physically inadequate to describe the phase-separation process of an Ising system.

The purpose of the present paper is to investigate the phase-separation process on fractals with infinite ramification order, such as the Sierpinski carpet family, for a nonconserved scalar order parameter. We expect the latter to be very sensitive to the presence of inhomogeneities in contrast with vector fields. The choice of a Sierpinski carpet has been suggested by the fact that it represents perhaps the simplest example of a nonstochastic fractal lattice, with infinite ramification order [5,10]. In Sec. II we introduce the Ginzburg-Landau (GL) model on the fractal lattice. In Sec. III we consider an auxiliary field approach [11] and discuss its asymptotic behavior. In Sec. IV we present numerical results of the exact equations of motion and monitor in several ways the growth process. In Sec. V, after stressing the similarities between the auxiliary field method and the spherical model, we draw the conclusions.

II. GINZBURG-LANDAU MODEL ON A FRACTAL LATTICE

We shall consider a scalar field ϕ_x whose properties depend on a standard Ginzburg-Landau free-energy functional and defined at every lattice cell, whose coordinate we represent by x:

$$H[\{\phi_x\}] = -\frac{D}{2}\sum_{i,j}\phi_x\Delta_{xy}\phi_y - \frac{r}{2}\sum_x^N\phi_x^2 + \frac{g}{4}\sum_x^N\phi_x^4, \quad (1)$$

where $r>0$ and $g>0$ are the quadratic and quartic couplings of the GL theory while the first term is proportional to the surface energy. We shall focus on the dynamical properties of the GL model on the two-dimensional deterministic Sierpinski carpet (SC) of fractal dimension (Hausdorff dimension) $d_f = \ln 8/\ln 3$.

In order to construct the SC, one divides a square lattice of $L \times L$ cells, with $L = 3^n$, into 3×3 blocks of equal size and the cells contained in the central block are discarded. Dividing again each of the remaining blocks into 3×3 subblocks and discarding all the central elements as many times as necessary to have the smallest subblocks constituted of a single cell, one obtains a structure of N cells, where $N = L^{d_f}$.

We make the assumption that the evolution towards equilibrium of the order parameter ϕ_x at the site x is given by the Ginzburg-Landau equation

$$\frac{\partial \phi_x(t)}{\partial t} = -\Gamma \frac{H[\phi(t)]}{\delta\phi_x(t)} + \eta_x(t). \quad (2)$$

Here $\eta_x(t)$ represents a Gaussian white noise with zero average and variance

$$\langle \eta_x(t)\eta_y(t')\rangle = 2T_f\Gamma\delta_{xy}\delta(t-t'),$$

where T_f is the temperature of the final equilibrium state, Γ is a kinetic coefficient, and δ_{xy} the Kronecker symbol.

By substituting Eq. (1) into Eq. (2) we find that ϕ_x, at any time after the quench, changes according to the equation

$$\frac{\partial \phi_x(t)}{\partial t} = \Gamma[D\Delta_{xy}\phi_y(t) + r\phi_x(t) - g\phi_x^3(t)] + \eta_x(t). \quad (3)$$

We shall write Δ_{xy} as a difference operator in analogy with the discrete representation of the Laplacian on Euclidean lattices. Periodic boundary condition are assumed, unless explicitly stated. The operator Δ is defined as $\Delta_{xy} = 1$ if x,y are nearest-neighbor cells, $\Delta_{xx} = -Z_x$, and $\Delta_{xy} = 0$ otherwise, where $2 \leq Z_x \leq 4$ counts the number of nearest neighbors of the site x.

At temperature $T_f = 0$, the free energy has two equivalent minima $\phi = \pm\sqrt{r/g}$. In the case of the spherical model we showed that the critical temperature vanishes when the spectral dimension is less than 2, while in the scalar case the critical temperature of a Sierpinski carpet is finite [12]. In the following, we shall concentrate on the dynamical properties for deep quenches $T_f \ll T_c$.

III. AUXILIARY FIELD APPROACH

In this section the so-called auxiliary field method [1,11,13], which has provided insight into the ordering dynamics of translationally invariant systems, will be applied to the nonconserved order-parameter dynamics on the Sierpinski carpet.

In this approach one replaces the physical field ϕ_x by an auxiliary field m_x, which varies in a smoother fashion across the interfaces and renders approximations feasible.

One chooses a nonlinear transformation from $\phi_x(t)$ to a new field $m_x(t)$ in such a way that the latter obeys an equation simpler than the original one. If such an equation is linear, the statistical properties of m_x are equivalent to those of free Gaussian fields and analytical work can be performed. Following the presentation of De Siena and Zannetti [11], one way of determining the transformation is to require that the auxiliary field linearizes the local part of the original equation of evolution [i.e., a zero-dimensional version of Eq. (3), obtained by setting $D = 0$]. For convenience, unless stated explicitly, we shall assume the stiffness constant D and the kinetic coefficient Γ to be 1. The auxiliary field m_x is introduced via the mapping

$$\phi_x = \phi(m_x) = \frac{m_x}{[1+(g/r)m_x^2]^{1/2}}. \quad (4)$$

In order to obtain the equation of motion for the auxiliary field m_x, we need to consider the nonlocal term

$$\sum_y \Delta_{xy}\phi(m_y) = \sum_{\langle y\rangle}\phi(m_y) - Z_x\phi(m_x), \quad (5)$$

where the sum $\sum_{\langle y\rangle}$ is restricted to the Z_x nearest-neighbors of the site x. Assuming that ϕ_x is a slowing varying function of m_x, one can expand the field at a nearest neighbor site y in a Taylor series

$$\phi(m_y) = \phi(m_x) + \phi'(m_x)(m_y - m_x) + \frac{1}{2}\phi''(m_x)(m_y - m_x)^2$$

$$+ (\text{higher-order terms}) \quad (6)$$

having indicated with primes the derivatives of ϕ_x with respect to m_x and neglected higher-order terms in the expansion. Collecting together the terms from the Z_x nearest neighbors one obtains

$$\sum_y \Delta_{xy}\phi_y \simeq \phi'(m_x)\sum_y \Delta_{xy}m_y + \frac{1}{2}\phi''(m_x)\sum_{\langle j \rangle}(m_x-m_y)^2. \tag{7}$$

The equation of motion for the auxiliary field m_x reads

$$\frac{\partial m_x(t)}{\partial t} = \sum_y \Delta_{xy}m_y + rm_x - \frac{1}{2}Q(m_x)\sum_y \Delta_{xy}(m_x-m_y)^2. \tag{8}$$

To obtain Eq. (8) we have used the identities

$$m_x = -\frac{-\phi(m_x)+g/r\phi(m_x)^3}{\phi'(m_x)} \tag{9}$$

and

$$\frac{\phi''(m_x)}{\phi'(m_x)} = -\frac{3(g/r)m_x}{1+(g/r)m_x^2} = -Q(m_x). \tag{10}$$

To proceed further, we consider a mean-field-like approximation for the last term in Eq. (8):

$$\sum_y \Delta_{xy}(m_x-m_y)^2 \simeq \frac{1}{N}\sum_{x,y}\Delta_{xy}(m_x-m_y)^2$$

$$= -2\frac{1}{N}\sum_{x,y}\Delta_{xy}m_xm_y. \tag{11}$$

Introducing the abbreviation

$$D_0(t) = -\frac{1}{N}\sum_{x,y}\Delta_{xy}m_xm_y, \tag{12}$$

the equation of evolution for the auxiliary field $m_x(t)$ reads

$$\frac{\partial m_x(t)}{\partial t} = \sum_y \Delta_{xy}m_y + rm_x - Q(m_x)D_0(t). \tag{13}$$

Upon neglecting the last term in Eq. (13), i.e., setting $Q(m)=0$, we recover the Kawasaki-Yalabik-Gunton theory [14]. Alternatively, we expand the function $Q(m_x) \simeq 3(g/r)m_x$ to first order in the coupling constant g and write [11]

$$\frac{\partial m_x(t)}{\partial t} = \sum_y \Delta_{xy}m_y(t) + \left[r - 3\frac{g}{r}D_0(t)\right]m_x(t). \tag{14}$$

The field m_x thus evolves according to an equation similar to the one found in the spherical model and in the Hartree-like approximation, the nonlinear term being treated self-consistently.

In order to obtain the properties of the field m_x we consider the eigenvalue problem

$$-\Delta_{xy}v_y^\alpha = \epsilon_\alpha v_x^\alpha, \tag{15}$$

where v_x^α is the xth component of the eigenvector associated with the eigenvalue ϵ_α of the operator Δ. There is an eigenvalue $\epsilon_0 = 0$ associated with the uniform mode whose eigenvector has all elements equal. The asymptotic behavior of the solution of Eq. (14) depends on the distribution of the smallest eigenvalues. After expanding the field m_x as a linear superposition of modes of amplitude $\tilde{m}_\alpha$,

$$m_x(t) = \sum_{\alpha=0}^{N-1}\tilde{m}_\alpha(t)v_x^\alpha, \tag{16}$$

one finds that each component evolves independently as,

$$\tilde{m}_\alpha(t) = \tilde{m}_\alpha(0)\exp[-\epsilon_\alpha t + B(t)]. \tag{17}$$

The quantity $B(t)$ must be calculated self-consistently from the governing equation (14):

$$\frac{\partial B(t)}{\partial t} = r - 3\frac{g}{r}\langle D_0(t)\rangle_0. \tag{18}$$

where the average $\langle\ \rangle_0$ is over the initial conditions of the field m_x. Using Eq. (12) and the eigenfunction expansion of $m_x(t)$, we compute $\langle D_0(t)\rangle_0$ as

$$\langle D_0(t)\rangle_0 = \frac{1}{N}\sum_\alpha \epsilon_\alpha|\tilde{m}_\alpha(0)|^2\exp[-2\epsilon_\alpha t + 2B(t)]. \tag{19}$$

For $N\to\infty$ a continuum density of states approximation $\rho(\epsilon) \simeq \rho_0\epsilon^{d_s/2-1}$ is appropriate and one can write

$$\langle D_0(t)\rangle_0 = A\int d\epsilon\rho(\epsilon)e^{-2\epsilon t + 2B(t)}, \tag{20}$$

where $\sqrt{A}$ is proportional to the amplitude of the fluctuations of the field m_x at the instant $t=0$. One ends with a closed equation for $B(t)$,

$$\frac{\partial B(t)}{\partial t} = r - 3\frac{g}{r}e^{2B(t)}A\int d\epsilon\rho(\epsilon)e^{-2\epsilon t}. \tag{21}$$

From Eq. (21) one sees that the quantity $B(t)$ must behave as

$$B(t) \sim \frac{d_s+2}{4}\ln t. \tag{22}$$

Thus, asymptotically the quantity $\langle D_0(t)\rangle$ goes to a constant value $r^2/3g$, while the equal-time correlation function diverges as

$$\frac{1}{N}\sum_x^N \langle m_x(t)m_x(t)\rangle_0 \sim t. \tag{23}$$

It is possible now to compute the correlation function

$$\langle m_x(t)m_y(t)\rangle_0 = A\int d\epsilon\rho(\epsilon)e^{-2\epsilon t + 2B(t)}v_x(\epsilon)v_y^*(\epsilon). \tag{24}$$

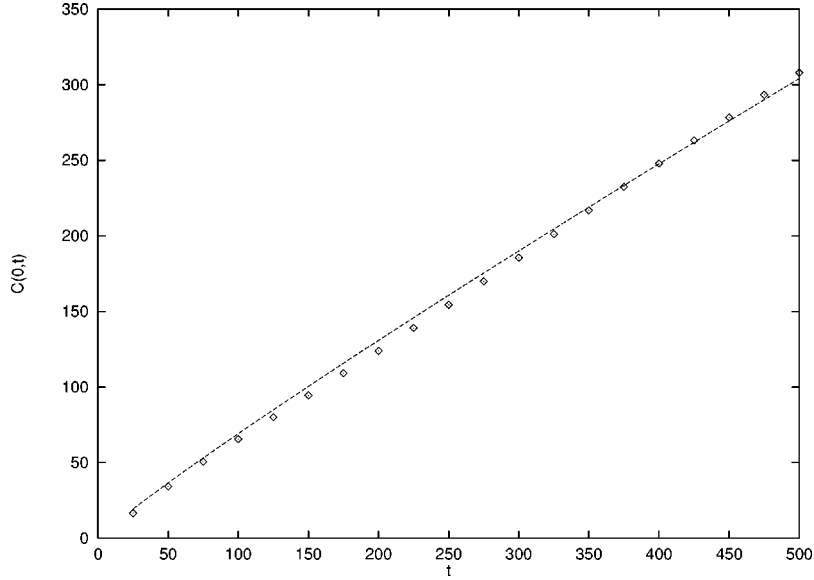A scaling form for the above quantity is (see [15])

FIG. 1. Peak of $C(0,t)$ (measured in r/g units), employing the auxiliary field method, plotted versus time in arbitrary units. The line represents the power-law growth $t^{d_s/2}$, with $d_s = 1.86$.

$$\langle m_x(t) m_y(t) \rangle_0 \sim t \exp\{-(R/t^{1/d_w})^{d_w/(d_w-1)}\}, \qquad (25)$$

where $R = |\mathbf{r}_x - \mathbf{r}_y|$ is the distance between the sites x and y. The above correlation function yields the following average value for the droplet size L as a function of time:

$$\langle L^2(t) \rangle \propto t^{2/d_w}. \qquad (26)$$

Knowing the evolution of the field $m_x(t)$, it is possible to determine the properties of the original field $\phi_x(t)$. Recalling that m_x has a Gaussian distribution at all times, one writes

$$P_m(m_x,t;m_y,t) = \frac{1}{Z_m} \exp\left\{-\frac{1}{1-\gamma^2}\left[\frac{m_x^2}{S_0(x)} + \frac{m_y^2}{S_0(y)}\right.\right.$$
$$\left.\left. -2\gamma \frac{m_x m_y}{[S_0(x)S_0(y)]^{1/2}}\right]\right\}, \qquad (27)$$

where Z_m represents a normalization factor

$$Z_m \equiv 2\pi \sqrt{S_0(x)S_0(y)(1-\gamma^2)}, \qquad (28)$$

with

$$S_0(x) \equiv \langle m_x^2(t) \rangle_0 \qquad (29)$$

and

$$G_0(x,y;t) \equiv \langle m_x(t) m_y(t) \rangle_0, \qquad (30)$$

$$\gamma(x,y) \equiv \frac{G_0(x,y;t)}{\sqrt{S_0(x)S_0(y)}}. \qquad (31)$$

The average value of the original field $\phi_x(t)$ can be calculated from

$$\langle \phi_x(t) \rangle = \int dm_x \int dm_y P_m(m_x,t;m_y,t)\phi(m_x), \quad (32)$$

while its correlator $G(x,y;t) \equiv \langle \phi_x(t)\phi_y(t) \rangle$ is given by

$$G(x,y;t) = \int dm_x \int dm_y P_m(m_x,t;m_y,t)\phi(m_x)\phi(m_y). \qquad (33)$$

Using the form of the distribution function P_m and Eq. (33), one finds for the correlation function of the ϕ field the result (see [13])

$$\langle \phi_x(t)\phi_y(t) \rangle = \int dm_x \int dm_y P_m(m_x,t;m_y,t)$$
$$\times \mathrm{sgn}(m_x)\mathrm{sgn}(m_y)$$
$$= \frac{2}{\pi}\phi_{coex}^2 \sin^{-1}[\gamma(x,y)]. \qquad (34)$$

Substituting Eqs. (23), (25), and (31) into Eq. (34), one obtains

$$\langle \phi_x(t)\phi_y(t) \rangle = \frac{2}{\pi}\phi_{coex}^2 \sin^{-1}[\exp-(R/t^{1/d_w})^{d_w/(d_w-1)}], \qquad (35)$$

which predicts a smooth decay of the correlation at long distances and the existence of dynamical scaling behavior in the late-stage growth.

To check the above results we have solved the equations of evolution (14) numerically on a Sierpinski carpet of size 243×243 and monitored the growth by measuring the fluctuation of the homogeneous component of the order parameter

$$C(0,t) = \frac{1}{N}\left(\sum_x^N \phi_x(t)\right)^2,$$

which is the zero component of the structure factor and grows in time, as shown in Fig. 1, with an apparent exponent $\nu = 0.93$, in agreement with the spherical model result [4],
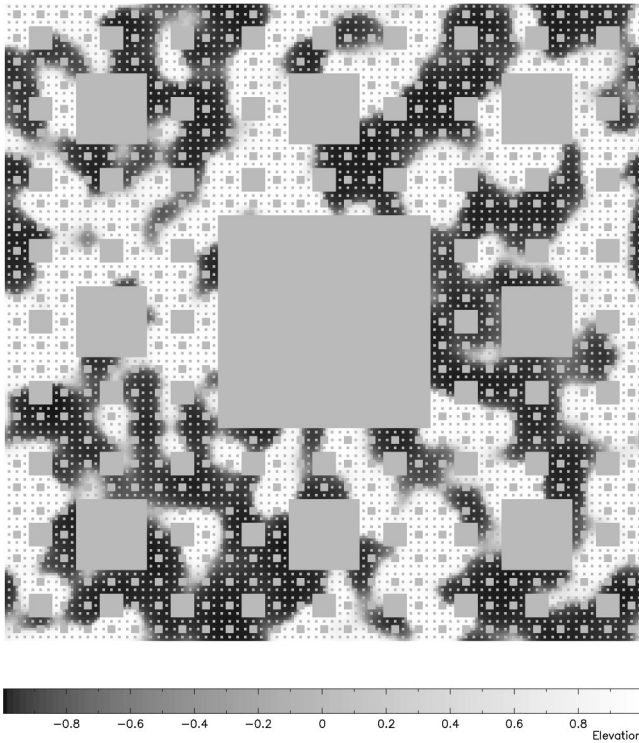
FIG. 2. Morphology of the domains obtained by solving numerically the equations for the auxiliary field method on a lattice 243×243. Notice that the droplet structure is not strongly affected by the presence of the holes, i.e., the interfaces are not pinned. The snapshot refers to times $t=25$ in the same arbitrary units as in Fig. 1.

which gives $\nu=d_s/2$, with $d_s=1.86$. The morphology of the field ϕ_x obtained by inserting the solution $m_x(t)$ into the nonlinear mapping (4) is shown in Figs. 2–4 and reveals the existence of large droplets growing in time in a fashion similar to that observed on compact supports, as if the fractality affects only the mass-to-size ratio of the domains, but does not suppress the diffusive motion of the walls. In this sense the auxiliary field method agrees quite well with the behavior of the spherical model. In the next section we shall compare these findings with a direct simulation of the Langevin equation.

IV. NUMERICAL RESULTS

We have investigated numerically the nonconserved dynamics on the Sierpinski carpet starting from a disordered state, generated assigning to each cell a random number uniformly distributed in the interval $[-0.125,0.125]$ and assumed $r=g=1$. In order to integrate numerically Eq. (8) we adopted a Euler discretization scheme with time step $\Delta t=0.01$ and Sierpinski carpets of different linear sizes $L=27,81,243$ with periodic boundary conditions. We have checked that our results do not change appreciably if we decrease Δt further. We also considered several temperatures quenches and runs up to $t=1000$. The averages for the various quantities presented below refer to 50 independent random initial configurations. In order to measure the droplet size we have applied the Hoshen-Kopelman algorithm [16]
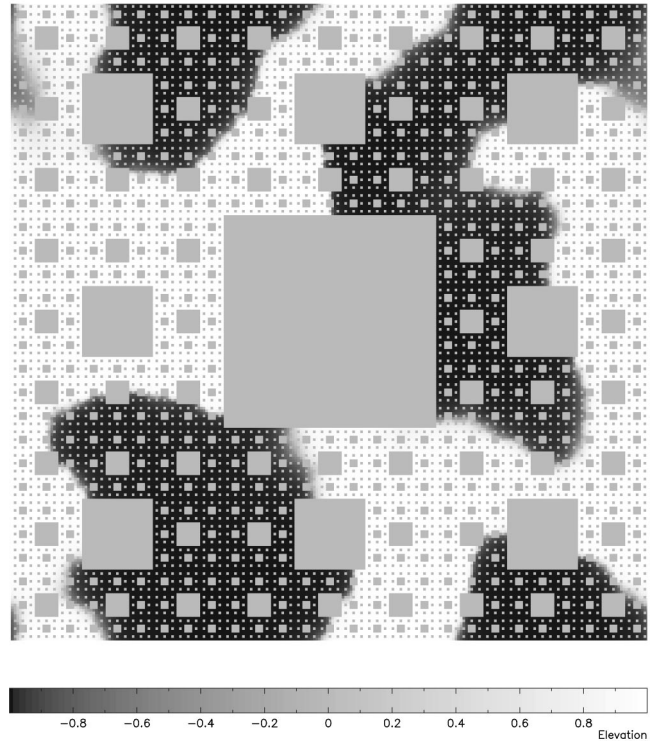

FIG. 3. Same as Fig. 2, but at $t=250$ (in arbitrary units).

to label the individual clusters formed by nearest-neighbor cells characterized by the same sign of the order parameter. Quantitative measures of the droplet properties are their masses and the radii of gyration. The mass M is defined as the number of cells belonging to a droplet, while the radius of gyration is defined as

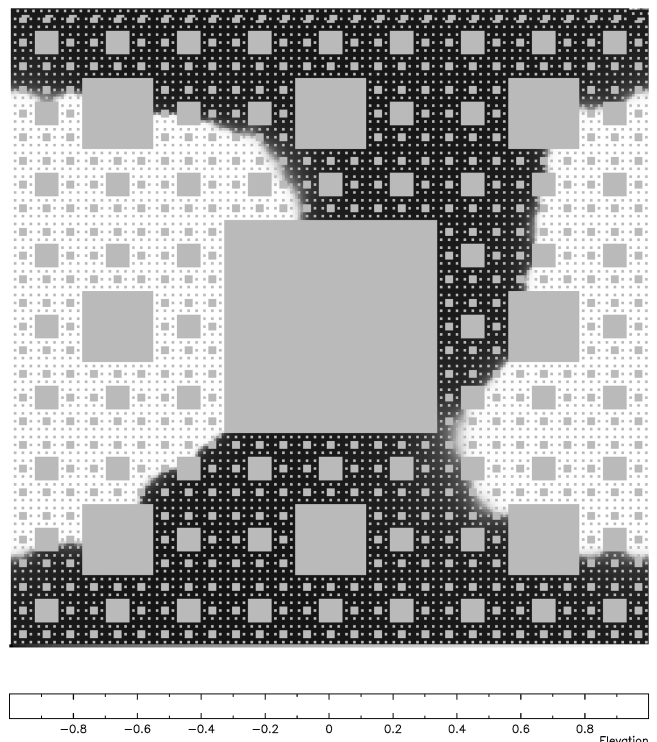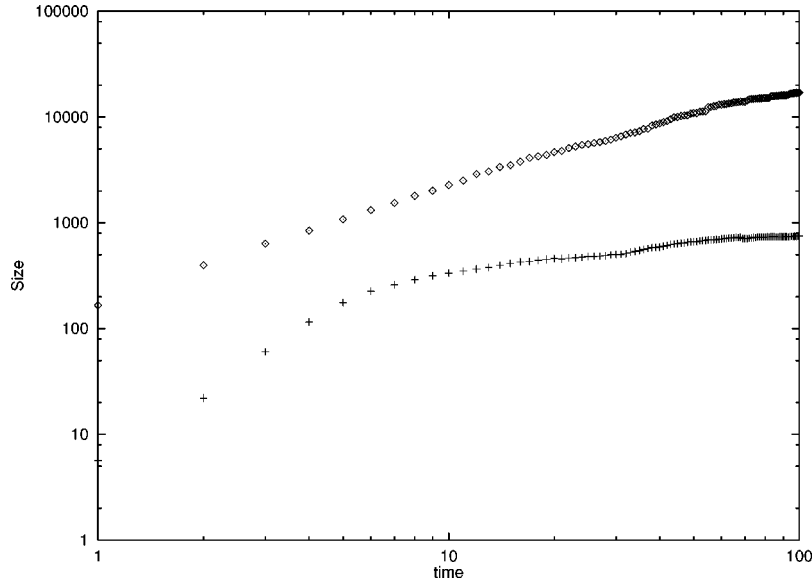FIG. 4. Configuration of the auxiliary field at $t=2500$ (in arbitrary units).

FIG. 5. Average size of the droplets (in lattice units) versus time t (in arbitrary units) calculated from the numerical solution of the Ginzburg-Landau equation. The data represent the averages over 50 sets of random initial conditions and noiseless dynamics $T=0$. The upper curve refers to a periodic system 256×256, while the lower curve to a Sierpinski carpet of size 243.

$$R^2 = \frac{1}{M}\sum_z^M \; [(x_z - x_{c.m.})^2 + (y_z - y_{c.m.})^2].$$

The sum is over the lattice sites belonging to a droplet, (x_z, y_z) is the position of the lattice sites z, and $(x_{c.m.}, y_{c.m.})$ is the position of its center of mass. To compute the mean value of $R^2(t)$ as a function of time we averaged over all droplets and over all initial configurations.

The growth law for the average size of the droplets is reported in Fig. 5 and the data are compared with those referring to a Euclidean square lattice of the same linear size. We observe that the growth is much slower in the first system than in the second. In Figs. 6–8 typical snapshots of the system are shown: The domain walls, separating opposite phases, sit on locations where the surface energy cost is lower and thermal fluctuations are needed to push the system out of these minima. Further evidence of the absence of power-law growth stems from the study of $C(0,t)$, which is compared in Fig. 9 with the corresponding quantity in the Euclidean case, known to grow as $t^{d/2}$.

Since in the late stage the characteristic width of the interfaces does not change appreciably with time, another independent measure of the domain structure is given by the ratio between the total number of sites and the number of sites N_p covered by interfaces, the so-called inverse perimeter density [17]:

$$P(t) = N_{sites}/N_p.$$

By assigning a perimeter site every time the absolute value of ϕ is less than the value 0.75, one obtains an estimate of P that is not too sensitive to the above threshold. While $P(t)$ displays power-law growth in translationally invariant structures and grows proportionally to $L(t)$, in the fractal case it saturates at a constant value for low-temperature quenches as shown in Fig. 10.

Another quantity with good self-averaging properties is the surface energy density (Fig. 11), whose time dependence we studied and compared with the Euclidean case. For compact supports this quantity decays as the inverse of the domain size $L^{-1}(t)$, while on the carpet it displays slow relaxation and eventually freezes.

Based on these results, one is led to the conclusion that, after the early regime, the average domain size and other
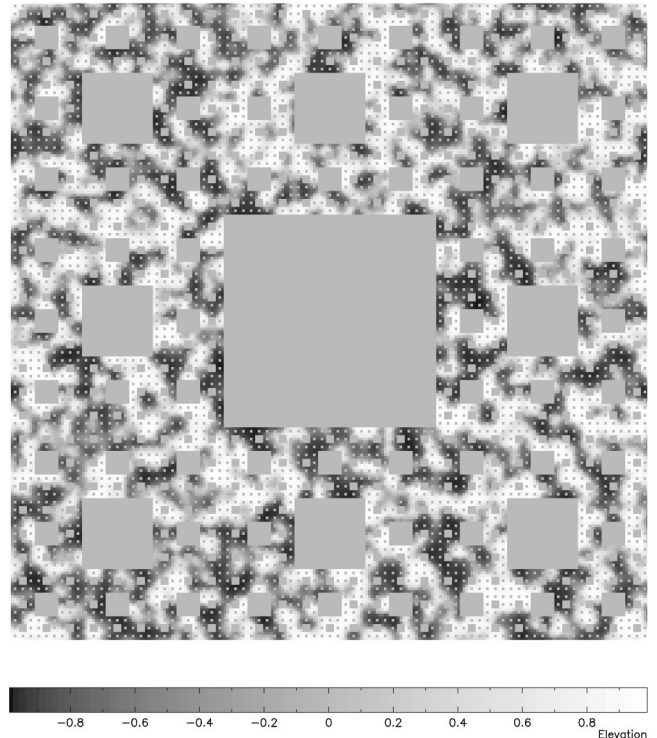

FIG. 6. Instantaneous configurations at $t=10$ (in arbitrary units) of the field obtained by solving numerically the Langevin equation on a Sierpinski carpet 243×243.
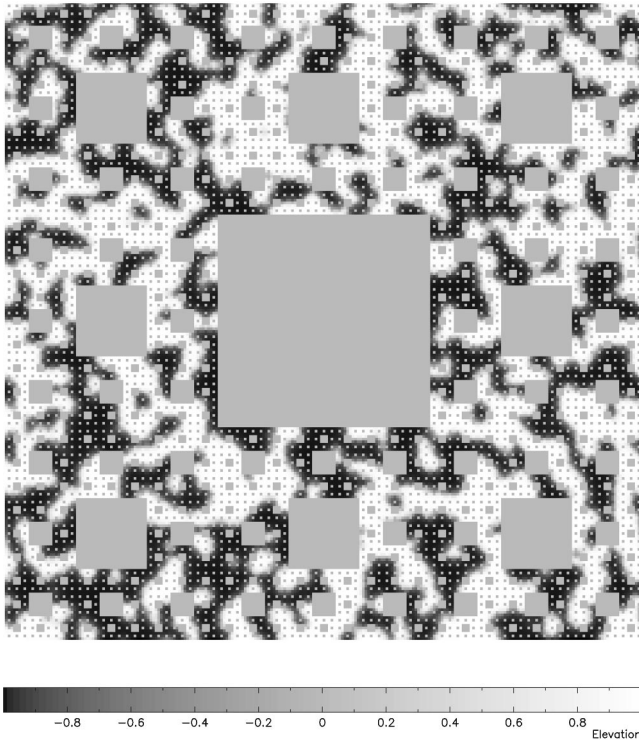
FIG. 7. Same as Fig. 6, but at $t = 100$ (in arbitrary units).

FIG. 8. Configuration of the scalar field at $t = 1000$ (in arbitrary units). Notice that the walls remain frozen at positions where the surface energy is at a local minimum.

indicators do not grow with a power-law behavior, as found in Euclidean lattices and in the spherical model on the same fractal support. At zero temperature one finds a breakdown of the self-similar dynamical scaling, in contrast with the compact case. Notice that the crossover from a diffusive and curvature driven dynamics to a thermally activated, Arrhenius-like, dynamics is not disorder induced as in the case of Ising diluted models [18–21]. During the early stage the domains coarsen almost linearly with time because the
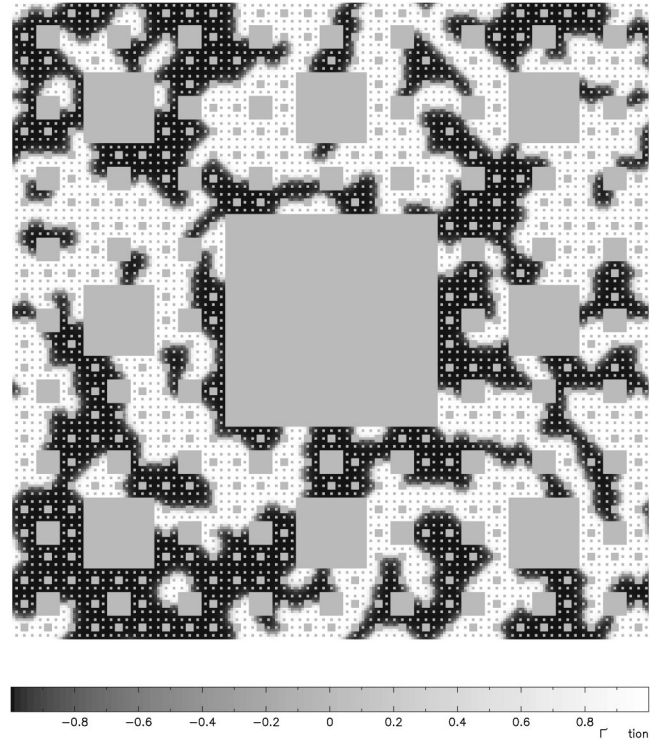
curvature provides the main driving mechanism, while at later times the growth becomes much slower and eventually stops since the height of the barriers that the domain walls have to surmount increases with the domain size. The dynamics selects configurations in which regions of opposite magnetization are separated by boundaries formed by a large number of voids. Since these configurations are associated
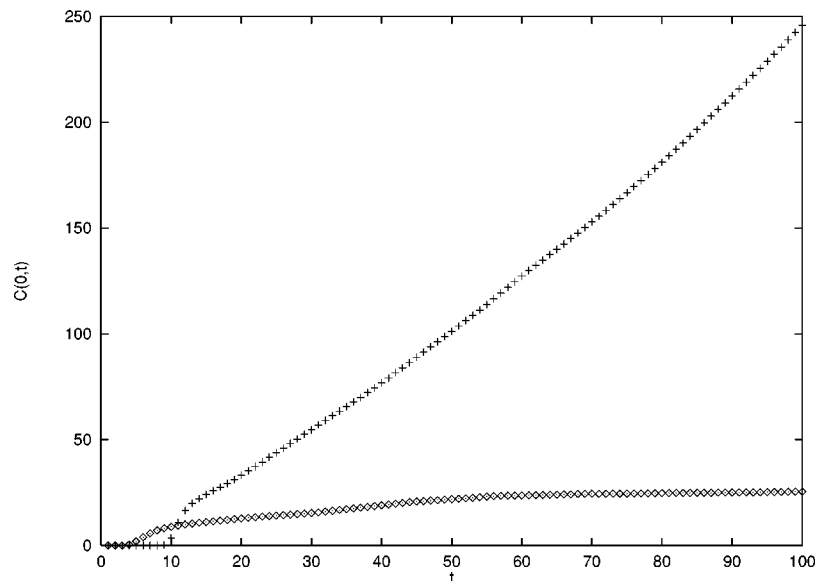

FIG. 9. Amplitude of the homogeneous component of the order-parameter fluctuation versus time (in arbitrary units) in the case of nonconserved scalar order-parameter dynamics on a Sierpinski carpet 243×243 (diamonds) and compact square lattice of the same size (crosses).
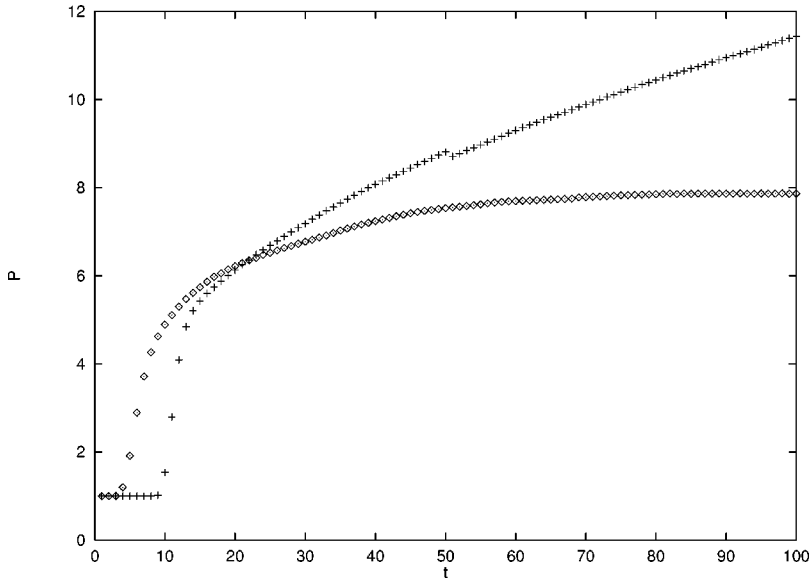
FIG. 10. Dimensionless inverse perimeter density versus time in arbitrary units for compact and fractal supports. The symbols are the same as in Fig. 9.

with low surface tension, the interfaces remain trapped.

Interestingly, the crossover time from a power-law growth regime, during which the trapping is not effective, to a frozen state is independent of the value of the stiffness constant D. This is understood by recalling that during the early stage the domain size grows diffusively as

$$R^2 \sim D t^{2/d_w}.$$

The pinning typically occurs when a moving interface encounters voids of size of the order of the interfacial width w, which scales as $w \sim \sqrt{D}$. Recalling that the distance between two voids of linear dimension w is proportional to w itself (due to the deterministic nature of the fractal), the typical separation of two domain walls is proportional to w. The asymptotic radius of the droplets is

$$R_\infty^2 \sim w^2 \sim D,$$

which gives a crossover time τ:

$$D \tau^{2/d_w} \sim D.$$

Therefore, the interfacial stiffness D determines the typical size of the droplets, but not the crossover time scale τ at which the freezing occurs.

Asymmetric, off-critical quenches lead to immediate equilibration of one of the two phases and fragmented patterns are not observed. On the other hand, when one considers the conserved order-parameter dynamics on percolation structures [24] even off-critical quenches fail to generate the
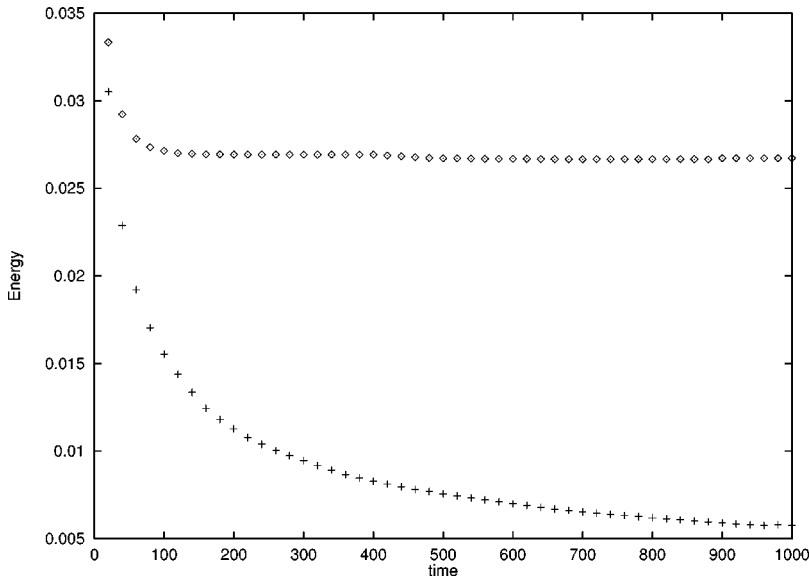

FIG. 11. Surface energy in arbitrary units as a function of time for a Euclidean lattice of size 256×256 and for a Sierpinski carpet 243×243. The symbols as in Fig. 9.
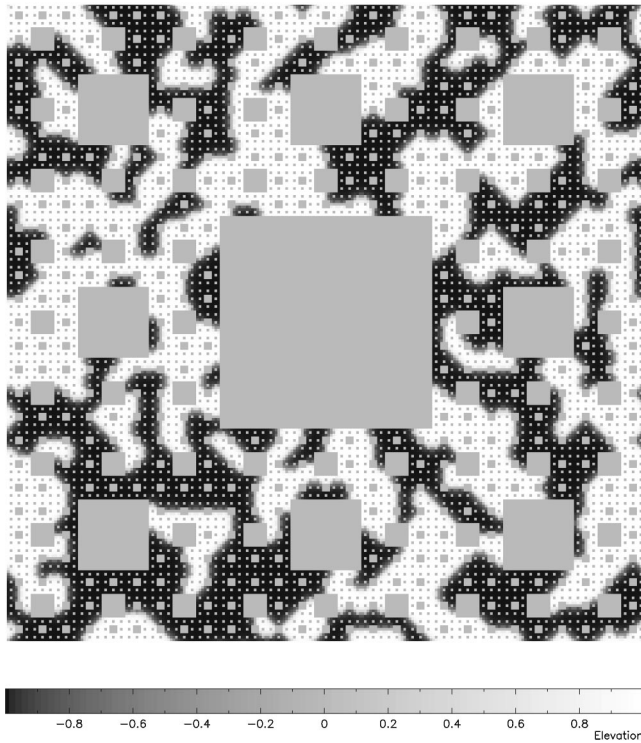
FIG. 12. Typical configuration obtained in the presence of twisted boundary conditions along the vertical direction at $t = 1000$ (in arbitrary units) for a Sierpinski carpet 243×243.

ordered state during a cooling at a reasonable rate and lead to frozen dynamic behavior with interrupted growth at low temperatures.

Twisted boundary conditions

We finally looked at the effect on the phase-ordering dynamics of a lattice with twisted boundary conditions along the x direction of the lattice, maintaining the periodicity

along the y direction. As $t \to \infty$ the compact system orders and forms two large domains of the opposite equilibrium phases, separated by rather sharp interfaces. On the contrary, on a fractal the system remains frozen in a highly fragmented structure, as shown in Fig. 12, because of the presence of voids, which reduce the role of the curvature. To characterize the interfacial roughness we consider the correlator

$$G(x) \equiv \frac{1}{N_y} \sum_y \phi(x,y) \phi(x,y) - \left(\frac{1}{N_y} \sum_y \phi(x,y) \right)^2,$$

where N_y represents the width of the system and the two arguments denote the longitudinal and transverse coordinates, respectively. In the case of the regular lattice, the peak of $G(x)$ narrows as the interface becomes straighter and sharper, while in the case of the fractal $G(x)$ remains multipeaked, as the interface pervades all the volume as illustrated in Fig. 13. One can go further by defining a characteristic width W of the interface as

$$W^2 \equiv \frac{1}{N_x} \sum_x x^2 G(x) - \left(\frac{1}{N_x} \sum_x x G(x) \right)^2.$$

As the time $t \to \infty$, $W(t)$ saturates to a much larger value than the corresponding quantity in a Euclidean lattice with identical boundary conditions and random initial conditions.

V. DISCUSSION AND CONCLUSIONS

On regular lattices, domain walls on sufficiently large scales can be approximated in the continuum limit by smooth curved interfaces, which either grow or shrink, whereas in the fractal case the background lattice has a pronounced influence on the phase separation. In a translationally invariant system the origin of the power-law-like behavior can be traced back to the interfacial motion: Immediately after the temperature quench, the system relaxes rapidly along the directions with the steepest gradients of the free energy and the order parameter sets locally to one its equilibrium values ϕ
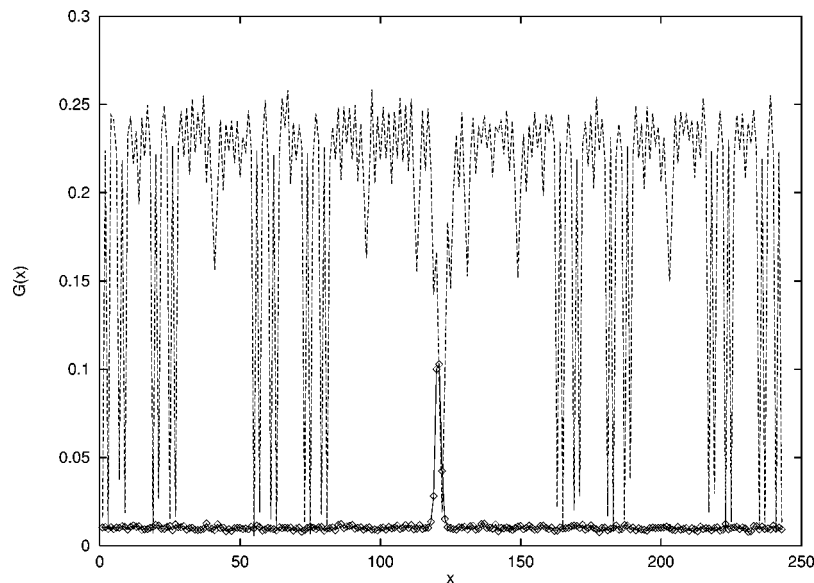

FIG. 13. Correlation $G(x)$ computed for a standard lattice (lines and points) and for a Sierpinski carpet (continuous line) with periodic boundary conditions along the x direction at time $t = 1000$ (in arbitrary units).
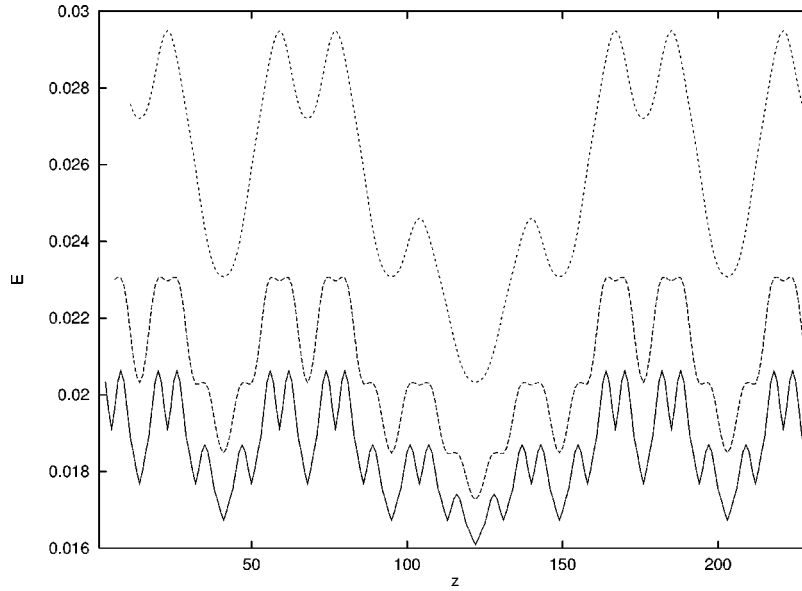
FIG. 14. Surface energy landscape, associated with a flat interface as a function of its location, for three different choices of the width of the interface. The continuous curve refers to an interface of width $w = 4$ in lattice units, the dashed curve refers to a curve of width $w = 8$, and the dotted curve refers to a diffuse ($w = 15$) interface. Notice the disappearance of small valleys as the interfacial width increases. The energy units are arbitrary and the x axis is in lattice units.

$= \pm \sqrt{r/g}$, leaving the system disordered, due to the presence of multiple domains of opposite phases separated by thin walls. This early regime is followed by a slower dynamics during which the driving force stems from the movement of the domain walls in order to reduce the interfacial energy. In other words, a curved portion of an interface will move and its velocity will be proportional to its local curvature, while a planar portion in the absence of thermal fluctuations comes to rest. The slow behavior of the late stage reflects the flatness of the energy landscape. One can think of the representative point of the system as moving along a direction characterized by a very small gradient of the free energy $H[\{\phi_x\}]$.

Let us consider the free-energy Hessian

$$\frac{\delta^2 H}{\delta \phi_x \delta \phi_y} = -\Delta_{xy} - [r \phi_x - 3g \phi_x^2] \delta_{xy}.$$

Its eigenvalue spectrum gives a measure of the stability of a selected configuration and reveals the origin of the slow directions of relaxation. If at a given time the configuration is close to one of the global minima of H, i.e., those characterized by uniform values of the field $\phi_x = \pm \sqrt{r/g}$, the spectrum contains only positive eigenvalues and the resulting relaxation process is an exponential function of time. On the other hand, a symmetric quench leads almost inevitably to the formation of a domain structure, which is associated with a saddle point and not to a minimum in phase space [22]. Thus the Hessian calculated in correspondence to the droplet solution must have a negative eigenvalue that corresponds to the expanding mode. The approach to equilibrium consists of the passage from the unstable droplet configuration to one of the absolute minima. Since the droplet size increases in time the free energy becomes flatter and flatter along the unstable path and the instability is reduced. Correspondingly, the as-

sociated negative eigenvalue vanishes, giving rise to a relaxation slower than any exponential function [23].

After this premise, we can see how the absence of translational invariance on a fractal support modifies all the features of the spectrum of fluctuations described above.

(i) The bulk fluctuations are modified and the system becomes more sensitive to thermal fluctuations because the density of state exponent d_s becomes smaller (less than d in fact). However, these modes remain stable since they correspond to positive eigenvalues of the Hessian.

(ii) The capillary wave spectrum, associated with a kink solution, will also be modified and the zero-mode Goldstone mode is suppressed by the following mechanism. Let us consider a rigid shift of a straight interface parallel to one of the directions of higher symmetry of the lattice. In Fig. 14 we show the the multivalley structure of the free energy, obtained by changing the location of the wall. A sequence of barriers hinders the normal fluctuations of the wall, which eventually serve to equilibrate the system in a standard lattice. This rugged landscape will determine a slower growth of the domains and instead of a diffusive motion in a homogeneous space the interface undergoes a diffusion in a system of barriers of varying heights.

(iii) The negative eigenvalue associated with the presence of a curved interface remains negative only for droplets of small size and becomes positive when the curvature energy becomes of the order of magnitude of the barriers.

Thus the role of the curvature energy, which provides the only driving force in translationally invariant systems, is greatly reduced because the lacunarity tends to pin the interfaces in configurations that locally minimize the energy. The residual dynamics can be understood in terms of consecutive transitions among metastable states, i.e., different basins of the free energy. Finally, at very low temperatures this mechanism eventually ceases and the dynamics becomes completely frozen.

Let us also remark that the multivalley structures are eliminated as the interfacial width exceeds the impurity size. Within the limit of infinite thickness one should be able to recover the results of the spherical model. In this model, in fact, the width of the walls increases in time during the ordering process; as a consequence one observes scaling. In contrast, in the scalar model the interfacial width W becomes asymptotically much shorter than both the domain size $L(t)$ and the voids, so that the system fails to show power-law growth.

The typical depth B of the local minima of the free energy can roughly be estimated to be proportional to the size of the domain L to some positive power ψ. The value d_f-1 is an upper estimate for the exponent ψ since the interfaces do not sit at random, but join places where the surface cost decreases.

Since the late-stage growth proceeds only via thermally activated processes, one can roughly estimate the typical time τ for a droplet of size L to overcome a barrier; this is given by the formula

$$\tau = \exp(B/k_B T_f) \sim \exp[(L(t)^\psi/k_B T_f].$$

Thus the domain size L evolves logarithmically as

$$L(t) \sim (k_B T_f \ln t)^{1/\psi},$$

in agreement with the droplet model [18], and stops completely at zero temperature because of the prefactor T_f.

To summarize, we have studied a simple nonrandom system and found that its late-stage behavior is not characterized by power laws and is not self-similar, as in the case of periodic substrates. We have also found that the treatment of the Ginzburg-Landau model on fractal substrates based on the auxiliary field method yields results that are consistent with the solution of the spherical model on the same support, but does not reproduce the phenomenon of pinning of domain walls, which is observed numerically. In fact, the spherical model fails to reproduce a necessary feature of phase-separating systems, i.e., domain walls of finite thickness. Moreover, contrary to the situation of the scalar model, within the spherical model there is no activation energy associated with the creation of a kink since the energy gap between the ordered phase and the instanton solutions vanishes in the infinite volume limit. This leads in the spherical model to a phase-ordering process that is diffusive and non-Arrhenius-like. The fractality of the substrate has the minor effect of rendering less effective the diffusive growth (because $d_w > 2$). Finally, the difference between the auxiliary field method and the numerical solution seems to be due to the mean-field assumption (11), which underestimates the effects of the inhomogeneous lattice.

ACKNOWLEDGMENTS

[1] A. J. Bray, Adv. Phys. **43**, 357 (1994). This represents a good review of the field.

[2] S. M. Allen and J. W. Cahn, Acta Metall. **27**, 1085 (1979).

[3] U. Marini Bettolo Marconi and A. Petri, Phys. Rev. E **55**, 1311 (1997); J. Phys. A **30**, 1069 (1997).

[4] U. Marini Bettolo Marconi and A. Petri, Philos. Mag. B (to be published).

[5] A lattice is said to be finitely ramified if upon eliminating a finite number of lattice bonds one can isolate an arbitrarily large subset of the infinite system.

[6] Y. Gefen, A. Aharony, Y. Shapir, and B. B. Mandelbrot, J. Phys. A **17**, 435 (1984).

[7] The exponent d_s relates the density of low-frequency states to the energy ϵ via the scaling formula $\rho(\epsilon) \sim \epsilon^{d_s/2-1}$.

[8] N. D. Mermin and H. Wagner, Phys. Rev. Lett. **17**, 1133 (1966).

[9] S. Alexander and R. Orbach, J. Phys. (France) Lett. **43**, L625 (1982).

[10] H.-O. Peitgen, H. Jurgens, and D. Saupe, *Chaos and Fractals* (Springer-Verlag, New York, 1993). The complexity of the Sierpinski carpet is considered in Chap. II.

[11] For a recent review of the auxiliary field methods see S. De Siena and M. Zannetti, Phys. Rev. E **50**, 2621 (1994).

[12] J. Ruiz, A. Tarancon, P. Carmona, and U. Marini Bettolo (unpublished).

[13] G. F. Mazenko, Phys. Rev. Lett. **63**, 1605 (1989); Phys. Rev. B **42**, 4487 (1990); **43**, 5747 (1991).

[14] K. Kawasaki, M. C. Yalabik, and J. D. Gunton, Phys. Rev. A **17**, 455 (1978).

[15] R. A. Guyer, Phys. Rev. A **32**, 2324 (1985).

[16] J. Hoshen and R. Kopelman, Phys. Rev. B **14**, 3428 (1976).

[17] T. M. Rogers and R. Desai, Phys. Rev. B **39**, 11 956 (1989).

[18] D. A. Huse and C. L. Henley, Phys. Rev. Lett. **54**, 2708 (1985).

[19] D. Chowdhury, M. Grant, and J. D. Gunton, Phys. Rev. B **35**, 6792 (1987).

[20] B. Biswal, S. Puri, and D. Chowdhury, Physica A **229**, 72 (1996).

[21] S. Puri, D. Chowdhury, and N. Parekh, J. Phys. A **24**, L1087 (1991).

[22] To see that a droplet is a saddle point consider the fact that it is stable with respect to bulklike fluctuations, i.e., with respect to uniform changes of the field ϕ_x, but unstable with respect to curvature fluctuations.

[23] A simple way of constructing ''saddles'' in phase space, separating the two uniform minima, has been proposed by J. Kurchan and L. Laloux, cond-mat/9510079. They divide the system into two pieces of opposite phases, separated by two straight interfaces at a distance h. The invariance of the system under translations and rotations determines the presence of soft modes, i.e., of excitations of the interfaces of vanishing energy cost. Thus the spectrum of the Hessian must contain a zero

eigenvalue associated with the existence of capillary wave massless modes, i.e., fluctuations of the interface about the straight configuration. This kind of fluctuation is marginally stable. One can see that the unstable direction corresponds to moving apart the two walls, a perturbation that is associated with the presence of a negative eigenvalue in the spectrum of the Hessian (however, exponentially small in the wall separation h).

[24] C. Castellano, A. Petri, and U. Marini Bettolo Marconi (unpublished).